



---

# THE POSSIBILITY OF USING A DIGITAL CAMERA AND VIDEOGRAMMETRIC TECHNIQUES FOR MONITORING OF OBJECTS MOVING AT DIFFERENT SPEEDS

**Fatin Mizher Radi**

Engineer, Technical College –AL-Mussaib (TCM),  
Furat Al-Awsat Technical University, IRAQ

**Dr. Jasim Ahmed Ali Al-Baghdadi**

Lecturer, Technical Engineering Surveying Dept.,  
Technical Engineering College –Baghdad (TCM),  
Middle Technical University (MTU), IRAQ

## ABSTRACT

*Over the past few years, some studies have introduced the capability of using a video camera and a videogrammetric technique in capturing the spatial changes in moving bodies. However, the previous studies have not evaluated the accuracy of tracking objects moving at different speeds. Thus, this research discusses of the feasibility of using a digital camera and a videogrammetric technique to capture spatial changes of objects moving at different speeds. The study includes validating the accuracy of a digital camera on videoing and tracking moving objects and determining effects of speed variations on the accuracy of monitoring moving objects.*

*A car (Mark KIA, SOUL) having many target points was chosen in this study to represent a moving object. The car was videoed at four circumstances (static and moving at speed (5km/h), (10 km/h) and (15km/h)) by two cameras mounted in two different angles to get stereo video clips. By utilizing videogrammetric technique, the stereo clips were used to determine the coordinates of target points placed on the car in the four circumstances. The accuracy of the work was evaluated by comparing the 3D coordinates of the targets determined using videogrammetry with the values of these points (control points) measured by total station. The assessment show that a digital camera are appropriate to achieve accurate and reliable measurement reach to millimeters when tracking a moving object at low speed (5km/h, 10km/h and 15km/h) and the videogrammetric technique can determine the spatial location of points on a dynamic object with total accuracy between (RMSE=  $\pm 2.00$  mm to  $\pm 4.00$  mm)).*

**Key words:** Videogrammetry, Monitoring moving objects, Video camera.

**Cite this Article:** Fatin Mizher Radi and Dr. Jasim Ahmed Ali Al-Baghdadi, The Possibility of Using a Digital Camera and Videogrammetric Techniques for Monitoring of Objects Moving at Different Speeds. *International Journal of Civil Engineering and Technology*, 9(8), 2018, pp. 318-331.  
<http://www.iaeme.com/IJCIET/issues.asp?JType=IJCIET&VType=9&IType=8>

---

## 1. INTRODUCTION

Over the past years, many researches have investigated the possibility of using new techniques for tracking moving objects. Some studies have introduced the ability of using a video camera and a videogrammetric technique in capturing the spatial changes in moving bodies [1-3]. Thus, videogrammetry includes all the techniques of using video images that are captured from different angles to track or create 3D models of mobile objects [3]. It provides very reliable and accurate measurements for different applications and it has been commonly utilized to offer non-contact precise 3D mapping for moving objects [4].

## 2. LITERATURE REVIEWS

The early studies about videogrammetry started at the end of 19th century by Muybridge and Marey to monitor the humans and animals locomotion [3]. A number of researchers have utilized a videogrammetry to analyze and track the motion of objects, humans or animals [1-10]. In case of analyzing human movement the reference [3] used a markerless videogrammetric technique to monitor and track a human movement. This technique does not require fixing any targets on a captured object. An optical motion capture system (MOCAP) was used to capture and analyze participant's movement. 3D surface models were produced to show the movement of the participant body. The accuracy of the measurements on this study was very good (within  $\frac{1}{4}$  pixel) [3]. In reference [4] a videogeammetry technique was applied and a single CCD video camera was used for measuring the vibrating modes of an airplane wing and the accuracy reach to sub-millimeters. The authors in reference [5] investigated the ability of using a high resolution video camera in digital photogrammetry on a shipyard to measure the coordinates of object points on the ship building industry. Some researchers in NASA in reference [6] used the videogrammetric technique on the solar sails. They prove that the possibility of using this technique in both static and dynamic cases. The researchers utilized two digital video cameras to generate sequences of series of three dimensional models of the Solar Sails. The RMS of the models and the proposed technique which have been extracted was very high (within sub-millimeter).

However, the previous studies have not assessed the accuracy of observing dynamic objects moving in different speeds and the relationship between object speed and the accuracy of the derived 3D coordinates of points on this object. Thus the purpose of this study is to assess the accuracy of the derived 3D coordinates of points on object moving in different speeds utilizing a videogrammetric technique. The study involves evaluating the validity of a commercial camera on videoing and tracking moving objects and the effects of the variation of object speed on the accuracy of observing and monitoring this object.

## 3. MATHEMATICAL ALGORITHM

Basically, the mathematical algorithm of videogrammetry involves the use of similar photogrammetric algorithms such as bundle adjustment which bases on collinearity equations ((1) & (2)). Bundle adjustment is an optimization method which is most widely used in image based scene reconstruction [11]. It incorporates observed image coordinates, exterior and intrinsic camera parameters as well as object space coordinates of the observed points. The

latter dominate the resulting nonlinear system. The collinearity equations, as the underlying mathematical model, incorporate observed image coordinates, exterior and interior camera parameters as well as object space coordinates of the observed points.

$$(x - x_p) + \Delta x = -f \frac{r_{11}(X-XL)+r_{12}(Y-YL)+r_{13}(Z-ZL)}{r_{21}(X-XL)+r_{22}(Y-YL)+r_{23}(Z-ZL)} \quad (1)$$

$$(y - x_p) + \Delta y = -f \frac{r_{31}(X-XL)+r_{32}(Y-YL)+r_{33}(Z-ZL)}{r_{31}(X-XL)+r_{32}(Y-YL)+r_{33}(Z-ZL)} \quad (2)$$

Where:

$(x,y),(x_p,y_p)$ : are image coordinates of an object and a principal point respectively.

$(\Delta x$  and  $\Delta y)$ : additional parameters obtained radial and tangential lens distortion.

$(r_n)$ : rotation matrix according to angles  $(\omega, \phi, \kappa)$ .

$(f)$  = principal distance (focal length) of a camera

$(X,Y,Z)$ ,  $(XL, YL, ZL)$ : are ground coordinates of object and principal point respectively.

#### 4. VIDEO CAMERA CALIBRATION

The interior orientation parameters of the camera (IOPs) are determined during camera calibration (focal length  $(f)$ , coordinates of principle points  $(x_c,y_c)$ , radial lens distortion, decentric lens distortion. These relative values of IOPs depend mainly on the nature of the camera [11].

To determine the IOPS, the collinearly equations are linearized according to the unknown (IOPs) parameters such as each camera lens centre coordinates  $(XL, YL, ZL)$ , each camera orientation  $(\omega,\phi,\kappa)$ , each lens distortion  $(K1,K2,K3)$ . In fact,  $K1$  is sufficient for medium accuracy. However, for precise photogrammetric applications or wide angles cameras the term  $K2$  and  $K3$  is required. In addition, each lens decentring  $(P1, P2)$  and each lens affinity and shear parameters  $(C1, C2)$  are determined using least squares techniques. This iterative computation process also determines the small corrections for the constants such as the principal distance  $(f)$  and the principal point  $(x0, y0)$  of the sensor chip. Once, these parameter values are determined 3D coordinates of point of interest are determined to fit the collinearity models

#### 5. EQUIPMENT AND DATA ACQUISITION SYSTEMS

The main equipment for research is two digital cameras (Nikon D5300 with resolution 16mega pixels), total station (TOPCON (GTS-750)) and invar scale bar as shown in Fig 1. The two cameras was utilized to capture a stereo video clips to a selected moving object (a moving car). A total station was used to measure 3D coordinates  $(x,y,z)$  of targets points which were fixed on and around the selected objects. A number of these targets were used as ground control points (GCP) while the others were employed as check points. Furthermore, an invar scale bar is always used to provide precise object-space scaling and to check the work accuracy.

The video mode of the camera was utilized to provide continues monitoring for objects, whereas the compact cameras were utilized to evaluate the measurement quality of the video cameras measurements. These cameras were suitable for capturing high resolution video clips. The main characteristics of this camera are illustrated as follow in Table 1.

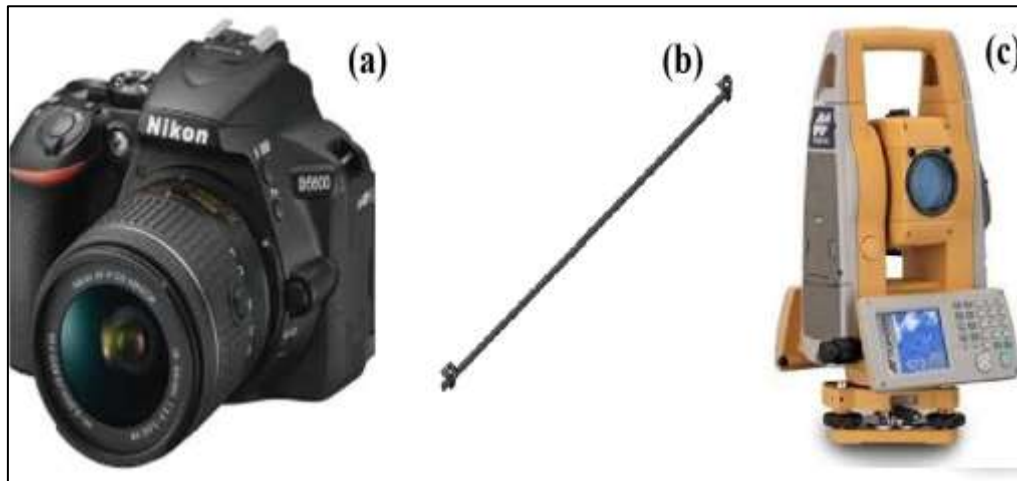


**Figure 1** Equipment of the study; (a) Canon camera (D5300), (b) Invar scale bar, (c) Total station TOPCON (GTS-750).

**Table 1** The characteristics of a Nikon camera.

Type	Compact digital camera	
Resolution	16 mega pixels	
Zoom	16-55 mm	
Image sensor size	23.5 x 15.6 mm CMOS sensor	
Image size (pixels)	Large:	6000 x 4000
	Medium:	4496 x 3000
	Small:	2992 x 2000
Speed shutter	1/4000 to 30in steps of 1/3 or 1/2 EV, bulb, times	
Weight	1kg	
Power supply	Battery	
Image type	JPEG, MOV	
Self-timer	2 s, 5 s, 10 s, 20 s	
Pixel size	0.0039mm	

## 6. SOFTWARE

In current time many software were used to process and analyze the video clips captured by cameras. These software are useful, efficient and time consuming. They also give the flexibility in analyzing the data. In this investigation two pieces of software were used:

a) **Virtual Dub**: is Internet freeware; it is used for video frame-grabbing and field de-interlacing software,

b) **PhotoModeler Scanner (PMS)**: this software is built in by Eos Systems Inc. Canada. It can be used for different photogrammetric and videogrammetric applications such as 3D point's measurements, 3D surface modeling using photos or video data [12].

## 7. RESEARCH METHODOLOGY

### 7.1. Camera Calibration

A calibration is an important step in photogrammetry especially when the work needed maximum accuracy. In this study PhotoModeler Scanner (PMS) software (2013) is adopted for achieving video camera calibration. The PMS software is designed especially for close range photogrammetry [4]. The method used in PMS calibration is optimized for the lens distortion to enhance the accuracy of image coordinates. A calibration process usually is fully

automated and do not required any intervention. PMS has a special calibration sheet designed to determine the interior parameters for used camera in each project. This sheet can be printed in two sizes ((8×11) inches or (36×36) inches).

A precise video camera calibration method was applied in this study to calibrate the cameras. The two Nikon cameras were calibrated twice using both images and video frames. For accurate results, the value of root mean square error (RMSE) needs to be not exceeding 1.0 pixel. Bundle adjustment method based on a collinearity approach is used for a camera calibration method. PMS software is adopted to calibrate the two cameras to determine the intrinsic parameters.

## 7.2. Videos Capturing and Processing

After cameras calibration processes, the cameras set up at appropriate distance from objects. The base/height was kept close to one in order to get precise stereo videos. Note, the base is the ground distance between the exposure stations of the two cameras while, the height is the ground distance between the camera and a captured object. The cameras were turned on to record the video clips for objects at same instance (approximately) from different angles to get appropriate stereo video clips. The recorded clips then uploaded to a computer for further processing.

Virtual dub software was utilized to convert the uploaded video clips to a series of video images. Then, the two synchronized stereo image from right and lift camera were selected visually for further processing. The preprocessing involves using PMS to determine of 3D-coordinates (x,y,z) of points placed on a car moving in different speeds. Fig 2 shows the cameras position according to the selected car that has many targets placed on. A car type KIA SOUL was used in this study.



**Figure 2** Targets and cameras positions

## 7.3. Frames Synchronization

Videogrammetry relies on the principals of photogrammetry. It is a technique usually used for monitoring dynamic objects. In order to get stereo photos from video clips, all used cameras have to be synchronized. Synchronization procedure normally applies to ensure that all selected cameras are recording video clips at the same time. Therefore; a low cost LED device was manufactured to provide video-frame synchronization.

There are many methods applied for video clips synchronization. Some methods use an audio signal or a controller device attached to cameras, while other methods give a signal to turn a camera on /off. In this investigation a synchronization technique bases on using an LED device which is similar to an approach introduced by reference [1]. This technique exploits a light flash near an object. Video cameras are synchronized by selecting the video frames which show the red flash on. Red light led fixed on a selected object was used to synchronize the two cameras. In fact, any mistake in selecting the right stereo frames will give improper results. This method considered the most common easiest in video clip synchronization compared to other synchronization methods. The light flash can be delivered by a small laser pointer or by turning on a LED s placed near the object. The red light flashes approximately every (0.133second).

### **7.3. Determining the 3D Coordinates of Targets Points**

A car (Mark KIA, SOUL) was chosen in this study to represent a moving object. A number of targets (12-bit type) were fixed on the car and on a closed static object (bridge) on a study area as shown in Fig 2 and Fig 3.a. Before videoing the car, the red light led was fixed on the car for cameras synchronization process and invar scale bar also fastened on the car to provide precise object-space scaling and to validate the accuracy of the results. The 3D ground coordinates of the target points were measured and determined using a total station TOPCON (GTS-750) with accuracy ( $\pm 1\text{mm}$ ).

In this study, the videogrammetric technique was used to determine the 3D spatial location of the target points when the car was static (Fig 3.a,b) and moving in three different speeds. Thus, the chosen car was videoed (four times) by the two cameras when the car was static and when it was moving at three different speeds ((5km/h), (10 km/h) and (15km/h)). The reasons behind that are to check the ability of a commercial camera on tracking moving objects in very slow and moderate speed and to analyze the effects of the speed variations on the accuracy of observing and monitoring moving object. Note, it is hard to track the car when it reaches a speed higher than (20km/h) because it is difficult to recognize the targets fixed on the car and they become gradually blurry as long as the car accelerating. Normally, the targets fade when the car reaching a speed higher than (20km/h) as shown in Fig 3.c.

In addition, the stereo video clips of both cameras of four car situations (static and moving at speed (5km/h), (10 km/h) and (15km/h)) were uploaded to the computer (PC) for further processing. Virtual Dub software was used to convert the stereo video clips of each car speed into stereo video images (stereo photo frames).

The stereo frames from left and right camera were synchronized visually in order to use them in PMS software for calculating 3D coordinates of the target points. The coded targets fixed on the bridge (a static object) were used as control points (CP). These CP were utilized primarily in PMS to achieve the orientation process and calculated the 3D coordinates of targets on the moving car. It is vital to ensure the produced 3D coordinates are precise and have low residuals.

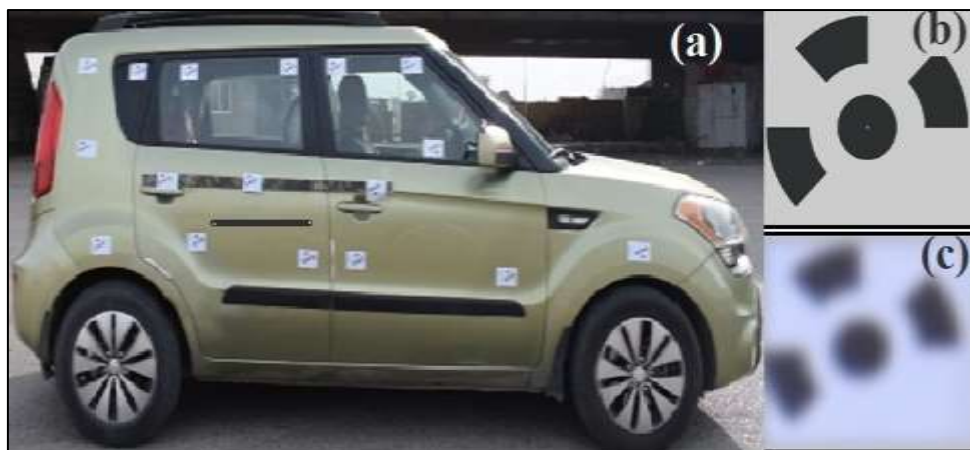


**Figure 3** Coded targets of points ; (a) Fixed targets on the car , (b) Clear target , (c) Blurry target

## 7.5. ACCURACY ASSESSMENT

Two accuracy assessment procedures were applied in this research to validate the results of videogrammetric approaches. The first assessment was achieved during the video camera calibration process. The procedure involves taking 12 very short videos (about 1 second) to the camera calibration sheet. Twelve photo frames extracted from the 12 videos (using Virtual Dub software) uploaded to PMS to perform a calibration process. Then, the PMS software showed a report which contains the overall camera calibration residuals and the calibrated inner orientation parameters of selected cameras.

The second assessment process includes evaluating the ability of a video mode in a digital camera on tracking moving objects and determining the effects of speed variations of on the accuracy of observing and monitoring moving objects. Thus, a number of CP and invar scale bare was chosen for this assessment process. Seventeen target points were used for assessing the accuracy of this study. The three dimensional coordinates of target points measured by total station with accuracy ( $\pm 1$  mm). They were considered as control points and free of errors. The stereo video images of the four car cases (static and moving at (5km/h), (10 km/h) and (15km/h)) were uploaded to PMS for determining the 3D coordinates of target points at each car speed. The accuracy assessment was done through comparing the 3D coordinates of the targets determined from PMS with the values of these points (control points) measured by total station. In addition, a precise invar scale bar (length 100 cm  $\pm 0.01$  mm) was utilized to evaluate the accuracy by comparing its true length with the length calculated from stereo images using PMS.

## 8. THE RESULTS

### 8.1. Camera Calibration

The selected cameras in this study were calibrated separately. As mentioned in Section (7.5), calibration procedure involves capturing 12 very short videos (about 1 second) by each camera to the camera calibration sheet. Twelve photo frames for each camera extracted from the 12 videos (using Virtual Dub software) uploaded to PMS to perform a calibration process. Then, the PMS software showed a report which contains the overall camera calibration residuals (RMSE) and the calibrated inner orientation parameters of selected cameras as shown in Table 2. The total residuals in the two cameras (1) & (2) were ( $\pm 0.217$  pixel and  $\pm 0.211$  pixel respectively). It is clear that all calibration residuals were under 1/2 pixel.



The parameters of the cameras ((1) & (2),(Nikon D5300)) used in this study are illustrated in Table 2.

**Table 2** Camera calibration parameters of the two selected cameras

Items	Camera Nikon D5300	
	Left camera	Right Camera
Focal length	4.654339 mm	4.651205 mm
(X <sub>0</sub> , Y <sub>0</sub> )	3.000049 mm × 1.676005 mm	3.001304 mm × 1.677754 mm
K1	4.859e-003	4.860e-003
K2	3.272e-005	3.327e-005
K3	0.000e+000	0.000e+000
P1	-5.864e-005	-6.713e-005
P2	1.676e-004	1.703e-004
No. of photos	12	12
Overall RMSE	0.217 pixels	0.211 pixels
Maximum RMSE	0.487 pixels	0.467 pixels

\* Total RMSE = (RMSE<sub>x</sub> + RMSE<sub>y</sub> + RMSE<sub>z</sub>)/3

## 8.2. 3D Coordinates Determination

As mentioned in Section (7.3), the 3D coordinates of targets points measured by a total station were considered a gold standard (free of errors). PMS was used to determine the 3D spatial location of target points fixed on the car from stereo video images when the car in four different circumstances (the car was static or moving at (5km/h), (10 km/h) and (15km/h)). The results of PMS (the 3D spatial location of target points) were compared with the results of the measurements of the total station. These results are illustrated in Tables 3, 4&5. The Tables 3 to 6 show that the Total RMSE\* in the measurements in the four circumstances (the car was static or moving at speed (5km/h), (10 km/h) and (15km/h)) were ±1.280 mm , ±2.549 mm, ±2.746 mm and ±4.002 mm respectively.

**Table 3** Measured, computed and residuals of the 3D GCP coordinates in circumstance one (the car was at static situation)

Points no.	Measured coordinates ( total station) (m)			Computed coordinates (with photo modeler) (mm)			Differences between coordinates (mm)		
	X	Y	Z	X	Y	Z	v <sub>x</sub>	v <sub>y</sub>	v <sub>z</sub>
1	2.7578	16.0096	21.3233	2756.064	16008.266	21323.2	1.74	1.34	0.1
2	2.7440	16.2761	21.3064	2742.911	16275.856	21305.8	1.1	0.25	0.6
3	2.7424	16.5471	21.3060	2740.149	16546.748	21305.6	2.26	0.36	0.4
4	2.7288	17.0517	21.3243	2728.665	17051.474	21323.7	0.13	0.23	0.6
5	2.7232	17.2778	21.3269	2720.854	17277.866	21326.7	2.45	0.06	0.2
6	2.7106	17.6530	21.3328	2710.321	17653.936	21333.4	0.28	0.94	0.6
7	2.7985	17.7749	21.0326	2801.64	17775.231	21033.1	3.14	0.33	0.5
8	2.9171	18.7417	20.6754	2902.79	18738.41	20677.1	14.31	3.29	1.7
9	2.8885	18.1159	20.5697	2888.657	18113.926	20570.4	0.15	1.9	0.73
10	2.9146	17.3950	20.6217	2915.319	17393.918	20621.7	0.72	1.08	0
11	2.9192	17.1587	20.6235	2919.924	17157.64	20624.1	0.72	1.06	0.6
12	2.9250	16.6169	20.6770	2922.776	16617.214	20676.6	2.22	0.31	0.4
13	2.9705	16.1259	20.6574	2972.153	16127.765	20657.3	1.65	1.86	0.1
14	2.8595	16.0182	21.0111	2859.279	16018.69	21010.1	0.22	0.49	1
15	2.9241	16.4515	20.8969	2923.877	16452.262	20896.7	0.22	0.76	0.2
16	2.9244	16.8777	20.8814	2925.045	16877.252	20881.2	0.64	0.45	0.2
17	2.9237	17.4735	20.8469	2923.577	17472.251	20846.7	0.12	1.52	0.2
RMSE*							3.343	0.835	0.413

$$* RMSE = \sqrt{\frac{\sum v^2}{n}}$$



**Table 4** Measured, computed and residuals of the 3D GCP coordinates in circumstance two (the car moving at speed (5 km/h))

Points no.	Measured coordinates (total station) (m)			Computed coordinates (with photo modeler) (mm)			Difference between coordinates (mm)		
	X	Y	Z	X	Y	Z	v <sub>x</sub>	v <sub>y</sub>	v <sub>z</sub>
1	2.7578	16.0096	21.3233	2751.24	16003.82	21327.08	6.55	5.8	3.78
2	2.7440	16.2761	21.3064	2737.78	16271.28	21309.17	6.22	4.8	2.77
3	2.7424	16.5471	21.3060	2738.58	16543.69	21307.55	3.82	3.41	1.55
4	2.7288	17.0517	21.3243	2725.51	17048.45	21324.89	3.29	3.24	0.59
5	2.7232	17.2778	21.3269	2726.58	17275.03	21327.08	3.38	2.77	0.18
6	2.7106	17.6530	21.3328	2710.58	17649.99	21333.66	0.01	3.9	0.86
7	2.7985	17.7749	21.0326	2798.79	17773.78	21033.46	0.29	1.11	0.87
8	2.9171	18.7417	20.6754	2929.10	18738.92	20674.86	12.01	2.8	0.54
9	2.8885	18.1159	20.5697	2888.5	18115.90	20569.70	0.00	0.00	0.00
10	2.9146	17.3950	20.6217	2908.19	17395.62	20621.59	6.41	0.6	0.11
11	2.9192	17.1587	20.6235	2909.60	17158.99	20624.11	9.6	0.29	0.61
12	2.9250	16.6169	20.6770	2919.13	16618.14	20678.31	5.86	1.24	1.32
13	2.9705	16.1259	20.6574	2962.76	16126.43	20658.56	7.74	0.53	1.16
14	2.8595	16.0182	21.0111	2850.69	16014.90	21012.54	8.81	3.31	1.45
15	2.9216	16.4510	20.9000	2921.6	16451.0	20900.00	0.00	0.00	0.00
16	2.9223	16.8775	20.9049	2918.31	16876.31	20899.70	3.98	1.19	5.19
17	2.9212	17.4741	20.8956	2918.49	17473.42	20887.01	2.71	0.67	8.58
RMSE							3.607	1.786	2.254

**Table 5** Measured, computed and residuals of the 3D GCP coordinates in circumstance three (the car moving at speed (10 km/h))

Points no.	Measured coordinates Using total station (m)			Computed coordinates Using PMS (m)			Difference between coordinates (mm)		
	X	Y	Z	X	Y	Z	v <sub>x</sub>	v <sub>y</sub>	v <sub>z</sub>
1	2.7578	16.0096	21.3233	2757.8	16009.6	21323.3	0	0	0
2	2.7440	16.2761	21.3064	2742.32	16275.22	21305.54	1.68	0.88	0.86
3	2.7424	16.5471	21.3060	2745.793	16547.04	21304.27	3.39	0.06	1.73
4	2.7288	17.0517	21.3243	2736.096	17049.77	21322.39	7.3	1.93	1.91
5	2.7232	17.2778	21.3269	2728.123	17274.46	21324.98	4.92	3.34	1.92
6	2.7106	17.6530	21.3328	2712.264	17647.66	21331.12	1.66	5.34	1.68
7	2.7985	17.7749	21.0326	2801.083	17772.44	21031.76	2.58	2.46	0.84
8	2.9171	18.7417	20.6754	2929.142	18736.44	20675.62	12.04	5.26	0.22
9	2.8885	18.1159	20.5697	2888.5	18115.9	20569.7	0	0	0
10	2.9146	17.3950	20.6217	2908.41	17396.97	20621.65	6.19	1.97	0.05
11	2.9192	17.1587	20.6235	2911.891	17162.06	20623.79	7.31	3.36	0.29
12	2.9250	16.6169	20.6770	2918.492	16622.47	20676.94	6.51	5.57	0.06
13	2.9705	16.1259	20.6574	2966.05	16134.33	20658.34	4.45	8.34	0.94
14	2.8595	16.0182	21.0111	2854.319	16020.56	21010.86	5.1	2.36	0.24
15	2.9216	16.4510	20.9000	2925.971	16457.05	20898.53	4.37	6	1.5
16	2.9223	16.8775	20.9049	2927.704	16881.79	20898.36	5.4	4.29	6.54
17	2.9212	17.4741	20.8956	2920.984	17473.8	20885.82	0.22	0.3	9.78
RMSE							3.162	2.474	2.602

**Table 6** Measured, computed and residuals of the 3D GCP coordinates in circumstance four (the car moving at speed (15 km/h))

Points no.	Measured coordinates ( total station) (m)			Computed coordinates (with photo modeler) (mm)			Difference between coordinates (mm)		
	X	Y	Z	X	Y	Z	v <sub>x</sub>	v <sub>y</sub>	v <sub>z</sub>
1	2.7578	16.0096	21.3233	2.7578	16.0096	21.3233	0	0	0
2	2.7440	16.2761	21.3064	2739.07	16273.58	21304.25	4.92	2.52	2.15
3	2.7424	16.5471	21.3060	2731.73	16543.07	21302.95	10.7	4.03	3.04
4	2.7288	17.0517	21.3243	2716.81	17045.63	21318.87	11.99	6.07	5.42
5	2.7232	17.2778	21.3269	2706.77	17270.25	21320.47	16.43	7.55	6.43
6	2.7106	17.6530	21.3328	2689.75	17643.81	21325.08	20.85	9.19	7.72
7	2.7985	17.7749	21.0326	2785.24	17770.54	21028.38	13.25	4.36	4.22
8	2.9171	18.7417	20.6754	2912.63	18738.96	20674.47	4.46	2.74	0.93
9	2.8885	18.1159	20.5697	2888.50	18115.9	20569.7	0	0	0
10	2.9146	17.3950	20.6217	2912.84	17396.76	20623.58	1.76	1.7	1.89
11	2.9192	17.1587	20.6235	2919.11	17162.16	20627.01	0.09	3.46	3.52
12	2.9250	16.6169	20.6770	2931.39	16622.97	20681.95	6.39	6.07	4.9
13	2.9705	16.1259	20.6574	2984.71	16135.93	20666.19	14.21	10.03	8.79
14	2.8595	16.0182	21.0111	2871.12	16026.04	21015.01	11.62	7.84	3.92
15	2.9216	16.4510	20.9000	2926.13	16454.66	20903.84	4.53	3.6	3.85
16	2.9223	16.8775	20.9049	2924.02	16880.17	20902.42	1.72	2.67	2.47
17	2.9212	17.4741	20.8956	2915.27	17473.26	20888.70	5.9200	0.84	6.89
RMSE							6.351	3.075	2.580

The target points placed on the car can be represented as 3D point as shown in Fig 4.a and the residuals in each target point can be displayed in linear shape as shown in Fig 4.b (Note , the value of the residual was magnified (700) time for demonstration purpose).



**Figure 4** 3D target point representation using PMS ; (a) 3D point model, (b) The residuals in target points

The results reveal that the residuals in the measurements increase as the speed of the moving car increases. Thus, the relationship between car speed and the values of the residuals can be represented in Fig 5. The figure displays the residual in each GCP point at three different speeds of the car (speeds (5km/h), (10 km/h) and (15km/h)). It is clear that the GCP have higher errors at speed (15km/h) as compared to other lower speeds (5km/h) & (10 km/h). Furthermore, figures (Fig 6, Fig 7& Fig 8) show the residuals at each axes (X,Y, &Z) in each GCP point of the four circumstances of the selected car (the car was static or moving at speed (5km/h), (10 km/h) and (15km/h)). The figures reveal almost axes X of the GCP have higher residuals compared to other axes. This mean increasing in car speed has significant impacts on reducing the accuracy of axis X compared to the other two axes.

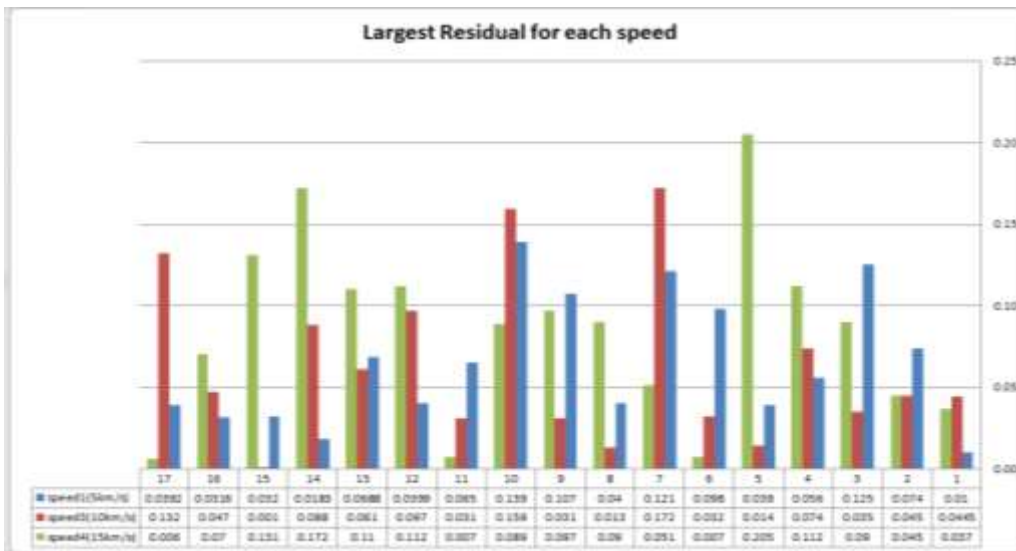


Figure 5 The residual in each GCP point at three different speeds of the car (speeds (5km/h), (10 km/h) and (15km/h)).

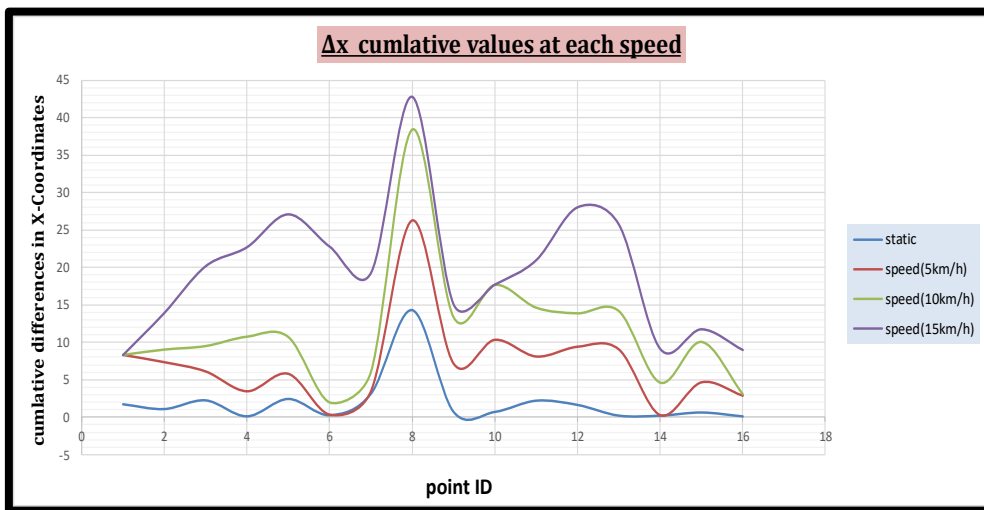


Figure 6 The residuals at axis (X) in each GCP point of the four circumstances of the selected car (the car was static or moving at speed (5km/h), (10 km/h) and (15km/h)).

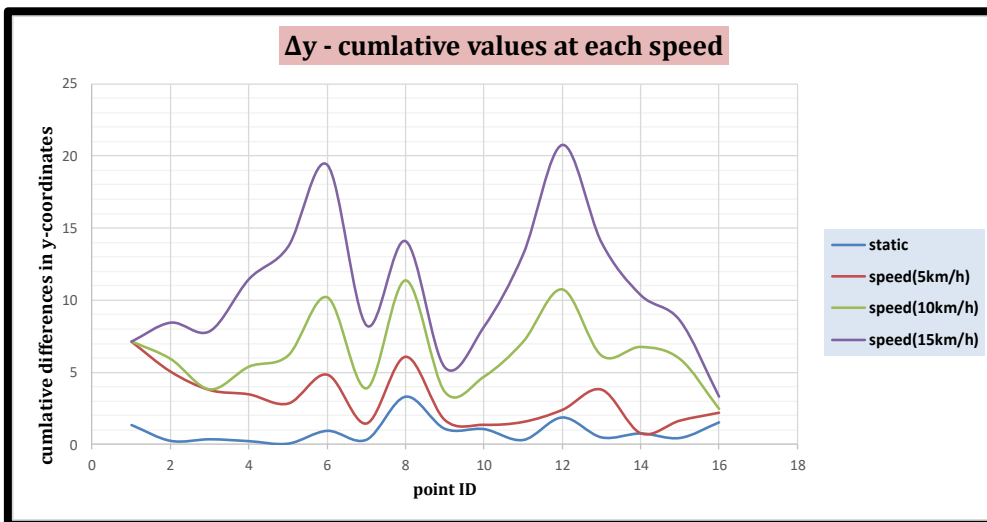
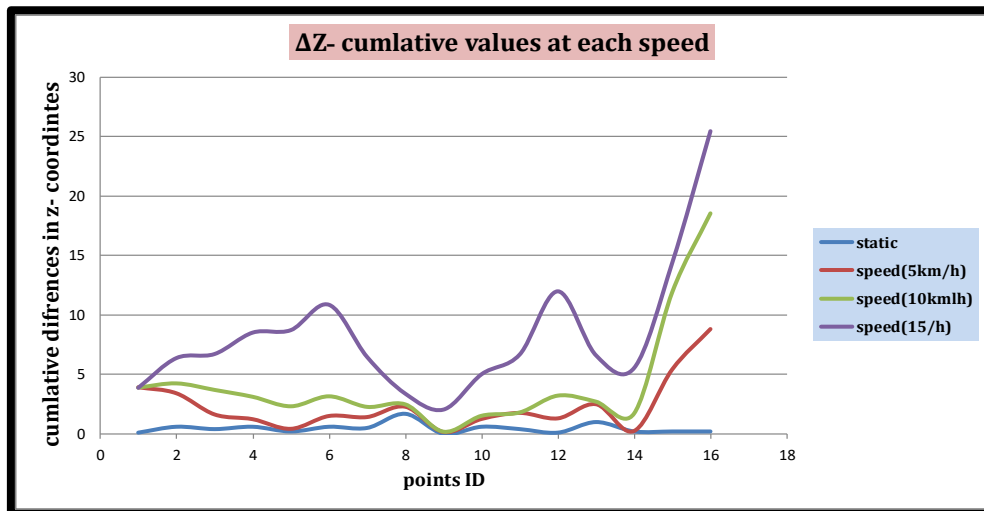


Figure 7 The residuals at axis (Y) in each GCP point of the four circumstances of the selected car (the car was static or moving at speed (5km/h), (10 km/h) and (15km/h)).



**Figure 8** The residuals at axis (Z) in each GCP point of the four circumstances of the selected car (the car was static or moving at speed (5km/h), (10 km/h) and (15km/h)).

### 8.3. Results Evaluations and Discussion

In this study, the accuracy assessment to the work was achieved in two stages. These stages are camera calibration and comparing the output results with the gold standard data (free of error data). The camera calibration results were shown in Table 2. The calibration results reveal that the residuals in the IOP of both cameras were too small (less than 0.3 pixel). These residuals were represented in a linear form (linear error) on grid points of the calibration sheet as shown Fig 9.a, b. It can be seen that errors decrease in the center and increase in the edges due to camera lens distortion. Thus, in this study the control points (GCP) were distributed regularly on whole study area (in center and edges) to reduce the lens distortion errors that may happen during videoing the car.

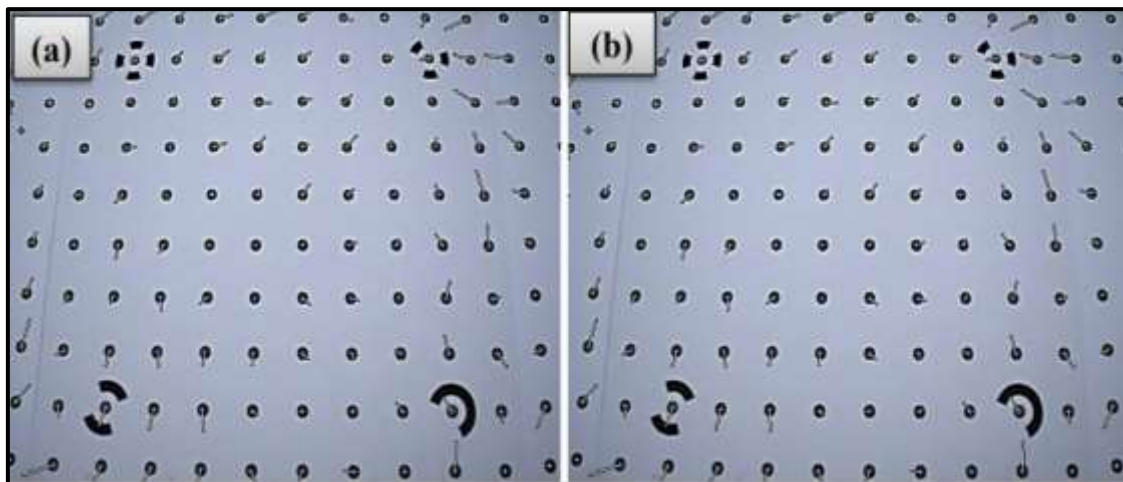


**Figure 9** The residuals in calibration grid points, (a) Left camera, (b) Right camera. Note, the residuals are magnified 300 times for demonstration purposes.

The second accuracy assessment produces were devoted to investigate the validity of a commercial camera on videoing and tracking moving objects and the effects of the variation of object speed on the accuracy of observing and monitoring this object. As stated in section (7.5), seventeen of GCP and invar scale bare was chosen for this assessment process. Tables 3 to 6 illustrate the results of comparing the 3D coordinates of the targets determined from PMS

(when the car static or moving) with the values of these points (control points) measured by total station. The Table 3 illustrates the total RMSE in the 3D coordinates of the derived target points on the parked car was small ( $\pm 1.530$  mm). However, the Tables 4 to 6 show the 3D coordinates and the RMSE in the derived target points on a car moving at three different speeds ((5km/h), (10 km/h) and (15km/h)). It is obvious that the RMSE in the in the derived coordinates increase with increasing the car speed. For instance, the total RMSE in the derived points on the car moving at speeds ((5km/h), (10 km/h) and (15km/h)) were  $\pm 2.549$  mm,  $\pm 2.746$ mm, and  $\pm 4.002$  mm respectively. Furthermore, the accuracy of the (X and Y) axes of the coordinates of the target points degraded significantly with increasing the speed of the car as compared with Z-axis coordinates.

In addition, a precise invar scale bar (length 100.000 cm  $\pm 0.010$  mm) was utilized to evaluate the accuracy by comparing its true length with the length calculated from stereo images using PMS. Table 7 illustrates that the residual in the length of the scale bar was -0.103 mm when the car was parking and the residual becomes -0.235 mm when the car was moving at speed (15 km/h). The results show the accuracy of the calculated length of the scale bar is affected significantly with increasing the speed of the car.

In brief, the results display that there is a direct relationship between the amount of the RMSE and the speed of the object. A digital camera is appropriate to achieve accurate and reliable measurement reach to millimeters when tracking a moving object at low speed (5km/h, 10km/h and 15km/h).

**Table 7** Comparing true length of scale bar with its lengths calculated from stereo images using PMS in four circumstances.

True length of the invar scale bar	Measured length of the scale bar fixed on the car when the car							
	Static		moving (5 km/h)		moving (10 km/h)		moving (15 km/h)	
	Length	$\Delta L^*$ mm	Length	$\Delta L$ mm	Length	$\Delta L$ mm	Length	$\Delta L$ mm
100.000 cm	100.103	-0.103	100.018	-0.018	99.987	0.013	100.235	-0.235

\*  $\Delta L = \text{True length} - \text{measured length}$

## 9. CONCLUSIONS

This study discusses the possibility of using a digital camera and videogrammetric techniques for monitoring of dynamic objects. The research involves evaluating the validity of a commercial digital camera on videoing and tracking dynamic objects and the effects of the variation of object speed on the accuracy of observing and monitoring this object. A car (Mark KIA, SOUL) was chosen in this study to represent a moving object. The chosen car was videoed (four times) by the two cameras when the car was static and when it was moving at three different speeds ((5km/h), (10 km/h) and (15km/h)). The results show that:

- A digital camera is appropriate to achieve accurate and reliable measurement reach to millimeters when tracking a moving object at low speed (5km/h, 10km/h and 15km/h).
- A videogrammetric technique can be used to determine 3D coordinates of points on moving object based on stereo video clips. The videogrammetric technique can determine the spatial location of points on a dynamic object with total accuracy between (RMSE=  $\pm 2.00$  mm to  $\pm 4.00$  mm).
- The results display that there is a direct relationship between the amount of the RMSE of the determined 3D coordinates and the speed of the object (RMSE increase with increasing object speed).

- A digital camera is not appropriate to video or monitor a dynamic object when it is moving at a speed higher than (20km/h) because it is hard to recognize the targets fixed on this object because they become gradually blurry as long as the object accelerating.

## REFERENCES

- [1] Chong, A., Al-Baghdadi, J., and Alshadli, D., 2014, High definition video cameras for measuring movement of vibrating bridge structure, International Conference on Vibration and Vibro-acoustics (ICVV2014), p(1-10).
- [2] Lee, C., and Faig, W., 1996, Dynamic monitoring with video systems, Photogrammetric engineering and remote sensing, vol.65, No.5, p(589-595).
- [3] Remondino, F., 2006, Videogrammetry for human movement analysis, Ninth international symposium on 3D analysis of human movement, p (1-5).
- [4] Ryall, T. and Fraser, C., 2002, Determination of Structural modes of vibration using digital photogrammetry, AIAA Journal of Aircraft, Vol. 39, No. 1, p(114-119).
- [5] Maas, H.G. and Hampel, U., 2006, Photogrammetric techniques in civil engineering material testing and structure monitoring, The Photogrammetric Engineering and Remote Sensing, Vol. 21, No.7, p( 29-45).
- [6] Black, J.T., 2003, Photogrammetry and Videogrammetry Methods Development for Solar Sail Structures, Prepared for Langley Research Center.
- [7] Hoviattalab, A.K., Rezaeian, T., Alizadeh, M., Bostan, M., Mokhtarzadeh, H., 2007, Design of a marker-based human motion tracking system, Biomedical Signal Processing Control, vol.2, p (59-67).
- [8] Lee, C.K., Faig, W., 1996, Vibration monitoring with video cameras, Int. Arch. Photogramm. Remote Sens, vol. 31, p(152-159).
- [9] Black, J.T., 2003, Photogrammetry and videogrammetry methods development for solar sail structure. Master's Thesis awarded by George Washington Univ.
- [10] Zhang, D., Guo, J., Lei, X. and Zhu, C., 2016, A High-Speed Vision-Based Sensor for Dynamic Vibration Analysis Using Fast Motion Extraction Algorithms. Sensors journal, vol., No.16, p(572).
- [11] Wolf, R., and Dewitt A., (2000). Elements of Photogrammetry with Application in GIS, 3rd edition, McGraw-Hill, New York
- [12] Photo Modeler Pro., (2008), User Manual Eos System Inc. Version 6.
- [13] Sanka Kruthi and Kamalakannan J, Implementation of Moving Object Detection and Categorization from HEVC Compressed Surveillance Video , International Journal of Mechanical Engineering and Technology , 9(4), 2018, pp. 35 – 42
- [14] M. Ramamoorthy, Dr. U. Sabura Banu, J. S. Praveen, P. Deepalakshmi and M. SRI RAM. An Efficient Real Time Moving Object Detection with Storage Reduction. International Journal of Computer Engineering and Technology, 6 ( 8 ), 2015, pp. 51 - 62 .